Full length article

Analysis and optimization for non-orthogonal pilot sequence sets in massive MIMO systems

Hong-Jae Lee [a], Dohyun Kwun [a], Sung Whan Yoon [a,b], Jin-Ho Chung [c,*,1], Seok-Ki Ahn [d]

[a] Department of Electrical Engineering, Ulsan National Institute of Science and Technology (UNIST), Ulsan, 44919, Republic of Korea
[b] Graduate School of Artificial Intelligence, UNIST, Ulsan, 44919, Republic of Korea
[c] Department of Electrical, Electronic, and Computer Engineering, University of Ulsan, Ulsan, 44610, Republic of Korea
[d] Media and Broadcasting Research Group, Electronics and Telecommunications Research Institute (ETRI), Daejeon, 44610, Republic of Korea

ARTICLE INFO

ABSTRACT

In modern wireless communication systems, orthogonal pilot signals has been generally employed in estimation of the channel state information. However, orthogonal pilot signals are inadequate for supporting the rapidly increasing requirements of communication throughput for 5G-and-beyond wireless environments, owing to the pilot contamination and short coherence times in high-mobility situations. To address these concerns, we present a new strategy for making use of non-orthogonal pilot sequences in channel estimation for multi-cell massive multiple-input multiple-output systems. First, we extend prior pilot assignment strategies based on the orthogonality of pilots to the general case of non-orthogonal pilot signals. Based on the proposed non-orthogonal pilot assignment strategy, we establish the minimal pilot length that fulfills a requirement for the channel estimate error, under a given degree of non-orthogonality. Then, we demonstrate validity of the pilot assignment strategy with the minimal length, which maximizes the entire network throughput. Simulation results show that our proposed method gives a significantly enhanced performance in terms of the net throughput compared to that with orthogonal pilot sequences. The performance gain becomes particularly significant with a higher density of users or shorter coherence time intervals.

1. Introduction

The increasing data consumption in mobile environments has promoted the rapid evolution of wireless communication technologies through the adoption of massive multiple-input multiple-output (MIMO) systems with multi-cell multi-user. Advanced communication schemes that can support a massive number of devices and provide a high quality of service (QoS) for large-scale data transmission must be developed. This arises from the exponential increment in the number of mobile devices per user and the corresponding requirements for large-scale data transmission. In addition, artificial intelligence (AI)-based systems and devices such as real-time surveillance systems, automated smart factory machines, and self-driving cars are likely to demand extremely high-performance data transmissions via 5G-and-beyond wireless communication systems in the future.

At the physical layer of modern wireless communication systems, massive MIMO is a core system for achieving a large communication capacity via multiple input and output antennas. The large number of antennas eventually mitigates the interference through independent fading channels of individual antennas [1–3]. Particularly, we may use a simple linear processor to take advantage of the massive MIMO approach due to the channel hardening property presented in [1]. However, due to the limited number of antennas, the channel hardening property is difficult to be ideal in practical scenarios. Therefore, to acquire channel state information (CSI) between a user equipment (UE) and a base station (BS), we employ pilot channel estimation with the channel hardening property. In a massive MIMO system, the CSI attained from the uplink pilot transmission can be utilized for channel estimation in downlink transmission within a coherence time, given channel reciprocity. Pilot sequences are utilized as signals in this way to estimate the channels of each user. A pilot sequence set can be viewed as a collection of complex vectors in the same dimension. In an orthogonal pilot sequence set, any two sequences are orthogonal in the sense of inner product of vectors. If the orthogonality is not satisfied, it is a non-orthogonal pilot sequence set. The magnitude of interference coming from signals transmitted by other users has a significant impact on

---

* Corresponding author.
  E-mail address: jinho@ulsan.ac.kr (J.-H. Chung).

how well channel estimation is performed. This effect is determined from the properties of the employed pilot signals. Thus, a suitable pilot sequence set should be adopted for the purpose of maximizing network capacity. An orthogonal sequence set has frequently been used as a pilot sequence set because two orthogonal pilot signals are easily separated from one another. For a multi-cell system, the simplest way to provide pilot sequences is to reuse a single orthogonal pilot sequence set for every cell [3]. Unfortunately, the deployment of small cells in 5G-and-beyond communication systems results in channel estimation interference between users who are using an identical pilot sequence, which is called *pilot contamination*. There are several known studies on mitigation of pilot contamination, which are based on precoding, spatial correlation, pilot design/coordination [3–18].

If fully distinct orthogonal pilot sequences could be distributed to all users in a multi-cell scenario, the contamination can be zero-forced. However, it is impossible since a larger number of orthogonal sequences requires pilot signals occupy a larger portion of the coherence time. The coherence time tends to be reduced in high-mobility situations, such as in vehicle communications. Previous studies with pilot design have focused on employing deliberate pilot reuse strategies to alleviate the pilot contamination effect while maintaining the orthogonality of pilot sequences. In [19,20], it was suggested to employ an optimization method for a hierarchical pilot reuse scheme that maximizes the overall network throughput. Specifically, they formulated the optimal pilot length N_{pilot} and reuse patterns of orthogonal pilot sequence sets for hexagonal multi-cell systems with a number of users per cell K, number of contiguous hexagonal cells L, and normalized coherence time N_{coh}. Another approach is to design a typical set of pilot sequence vectors that alleviates the pilot contamination effect by considering orthogonal as well as non-orthogonal cases. In [5], the authors designed complex-valued non-orthogonal pilot sequences with minimum mean-squared errors (MMSE) by solving the line packing problem on a complex Grassmannian manifold. In their work, the variance of the channel estimation error is calculated, and a design criterion of non-orthogonal pilot sequences that minimizes the channel estimation error is given. In [6], the authors proposed a generalized Welch-bound-equality sequence design-based approach to produce non-orthogonal pilot signals. The algorithm returns a pilot design achieving the user capacity, where the capacity is the maximum number of users in the overall multi-cell system that satisfies the given signal-to-inference-plus-noise ratio (SINR) requirements in downlink transmissions. Recently, in [17], the authors suggested a coordinated pilot sequence optimization method across multiple cells based on fractional programming.

In this study, we focus on an optimal pilot reuse strategy that maximizes the capacity over entire systems when non-orthogonal pilot sequence sets are adopted. For orthogonal pilot cases, only the interference from other cells that reuse the same pilot sequence determines the pilot contamination effect. By contrast, for non-orthogonal cases, more users can be supported using distinct non-orthogonal pilot sequences, but all other users with non-orthogonal pilot signals interfere with the channel estimation. Therefore, the optimal pilot reuse strategy across multiple cells for non-orthogonal pilot cases is quite different from that for orthogonal cases. Our main contributions can be summarized as follows:

- We formulate a certain condition for reducing the MSE in channel estimation with the non-orthogonal sequences, then derive a minimal length of the non-orthogonal pilot signals to satisfy the MSE condition.
- We determine the optimal pilot reuse pattern that maximizes the net-sum rate of the overall system.

- Via extensive simulation results, we demonstrate that the pilot reuse strategy employing the non-orthogonal pilot sequence sets shows a growing gain in total net-sum rates as compared to the orthogonal pilot reuse strategy as the user density increases and the coherence time shrinks. In particular, the non-orthogonal pilot set shows a net sum rate per user significantly greater than that of the orthogonal pilot set when the normalized coherence time is less than 90 and the number of users is greater than 10.

The organization of the manuscript is as follows. In Section 2, we explain the multi-cell massive MIMO system model. In Section 3, we study the optimal pilot assignment strategy in [19,20] with orthogonal pilot signals, and derive the MSE of channel estimation as well as the net-sum rates in the non-orthogonal case. We derive the pilot assignment vector and the minimal length of the non-orthogonal pilot signals in Section 4. We present some simulation curves on the net throughput in Section 5. We finally discuss some concluding remarks in Section 6.

2. System model

We assume a multi-cell massive MIMO system with one BS and M antennas per cell to accommodate K independent users with a single antenna. Except for the cell to which they are allocated, users in all L cells can interfere with one another. When the channel reciprocity is maintained, the channel vector $\boldsymbol{h} \in \mathbb{C}^{M \times 1}$ represents the CSI between a BS and a user. We denote the small-scale fading factor as $\boldsymbol{g} \in \mathbb{C}^{M \times 1}$, and the large-scale fading factor as $\sqrt{\beta}$. The channel vectors for uplink and downlink within the coherence time are denoted by $\boldsymbol{h}$ and $\boldsymbol{h}^{\mathrm{H}}$, respectively, where $\boldsymbol{h} = \sqrt{\beta}\boldsymbol{g}$, and H represent the Hermitian of a vector. In Fig. 1, the CSI between the kth user in the ith cell and the BS in the lth cell is denoted by $\boldsymbol{h}_{li_k}$. Moreover, the received signal $Y_{l_t} \in \mathbb{C}^{M \times \tau}$ at the tth target user in the lth cell is given as follows:

$$Y_{l_t} = \sqrt{\frac{\rho_0}{\tau}} \sum_{i=1}^{L} \sum_{k=1}^{K} \boldsymbol{g}_{li_k} \sqrt{\beta_{li_k}} \phi_{i_k} + W_{l_k} \tag{1}$$

where $\boldsymbol{g}_{li_k}$ is the small-scale fading factor from the kth user at the ith cell to the BS in the lth cell, and $\sqrt{\beta_{li_k}}$ is the large-scale fading factor from the kth user at the ith cell to the lth cell. Note that $\boldsymbol{g}$s are considered to be independent and identically distributed according to the characteristic of massive MIMO systems. Besides, ρ_0 denote the signal power, τ is the pilot signal length, $\boldsymbol{\phi}_{i_k} \in \mathbb{C}^{1 \times \tau}$ represent a pilot signal vector for the kth user in the ith cell. The additive white Gaussian noise matrix is also expressed as $W_{l_t} \in \mathbb{C}^{M \times \tau}$, for the tth user in the lth cell. If we denote the coherence time as T_{coh} and the delay spread as T_{del}, then we have $N_{coh} = T_{coh}/T_{del}$, which is called the normalized coherence time by delay spread, and is a measure to assess the performance of a communication system under a variety of channel conditions.

From [21], it is known that the signal-to-interference ratio at the tth user in the lth cell during downlink data transmission, can be written as

$$SIR = \frac{\beta_{ll_t}^2}{\sum_{i \neq l} \beta_{li_t}^2} \tag{2}$$

when M goes to infinity, under use of orthogonal pilot signals.

3. Pilot analysis

In this section, backgrounds and strategies in [5,19,20] will be firstly reviewed. Then, those will be combined with the characteristics of non-orthogonal pilot sequences to derive network throughput under the assumptions in massive MIMO systems.
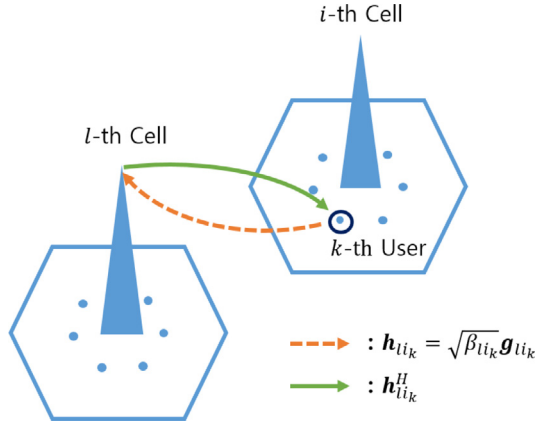
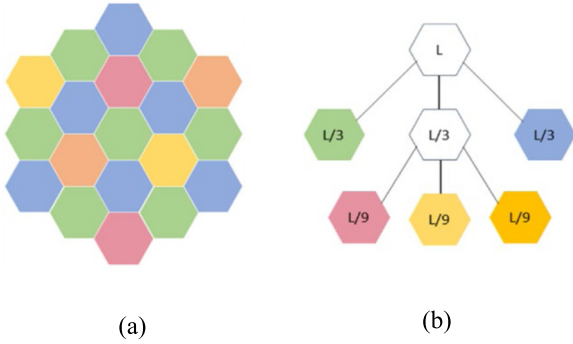**Fig. 1.** Interfering cells with uplink and downlink.

Fig. 2. Three-division pilot assignment.

3.1. Pilot assignment in massive MIMO

We suppose that pilot signals are obtained from the τ-dimensional complex sphere line packing method [5]. In general, the effect of pilot contamination can be measured in terms of inner product of two vectors. Clearly, the number of distinct non-orthogonal sequences are more than the number of distinct orthogonal sequences within the space of same dimension. For instance, only three orthogonal vectors ($\theta = 90°$) can be picked up on the 3-dimensional sphere, while four more points with $\theta = 45°$ can be selected. Let ϕ_A and ϕ_B be two vectors of pilot signals for users A and B, respectively. The non-orthogonality between ϕ_A and ϕ_B is given by

$$\phi_A \cdot \phi_B = \tau \cos\theta_{AB}, \tag{3}$$

where θ_{AB} is the angle between the two pilot vectors. Note that $0 \leq \phi_A \cdot \phi_B \leq \tau$. Therefore, $cos\theta_{AB}$ can be used to illustrate the effect of pilot contamination.

We employ the three-division strategy in [19,20] for pilot assignment. As in Fig. 2, L cells consist of units of three cells that locate with the same grid distance. In Fig. 2a, a pilot signal set is shared by cells with the same color. The tree structure with three division in Fig. 2b shows the grid distance among cells based on the depth. A vector $\boldsymbol{p}$ is defined to represent the pilot assignment state to examine the impact of pilot contamination by different cell clustering states. We also use K single-user pilot assignments over L cells, in which there are as many tree structures as there are users for the single-user situation with L cells. The valid set of pilot assignment vectors generated from the three-division

strategy can be written as

$$P_{L,K} = \left\{ \boldsymbol{p} = (p_0, p_1, \ldots, p_{\log_3 L-1}) : 0 \leq p_d \leq K3^d, \sum_{d=0}^{\log_3 L-1} p_d 3^{-d} = K \right\}, \tag{4}$$

where p_d is the pilot reuse factor which means number of cells at depth d. Let $N_{op}(\boldsymbol{p})$ denote the length of the orthogonal pilot sequence given the pilot assignment vector $\boldsymbol{p}$, which is written as

$$N_{op}(\boldsymbol{p}) = \sum_{d=0}^{\log_3 L-1} p_d. \tag{5}$$

Note that $N_{op}(\boldsymbol{p})$ can be also considered as the number of distinct sequences in the pilot signal set. In [20], the assignment vector $\boldsymbol{p}$ which maximize the network capacity is given as

$$p_d = \begin{cases} \sum_{s=0}^{d} K3^s - \frac{N_{op}(\boldsymbol{p})-K}{2}, & d = x \\ 3\left(\frac{N_{op}(\boldsymbol{p})-K}{2} - \sum_{s=0}^{d-2} K3^s \right), & d = x+1 \\ 0, & \text{otherwise} \end{cases} \tag{6}$$

where $x = \min\left\{ k | \sum_{s=0}^{k} K3^s > \frac{N_{op}(\boldsymbol{p})-K}{2} \right\}$. Similarly, we define $N_{np}(\boldsymbol{p}_\tau, \tau)$ as the number of distinct non-orthogonal pilot sequences whose lengths are τ, where $\boldsymbol{p}_\tau$ is the pilot assignment vector for the non-orthogonal cases. In Section 4, we will investigate the effect of $N_{np}(\boldsymbol{p}_\tau, \tau)$ for $\boldsymbol{p}_\tau$, and compare resultant performances with the orthogonal cases.

3.2. Channel estimator based on MMSE

Under use of non-orthogonal sequences as pilot signals, there exist some interferences caused by non-orthogonality among pilot sequences. To evaluate the impact of such interferences to the quality of channel estimation, we need to adopt some metric. We select the minimum mean square error (MMSE) estimator. It was shown that in the comparison of the performance of channel estimation, MMSE achieves the best performance for channel estimation [22]. The MSE and inner products between the real and the estimated channels represent the estimated channel with pilot contamination.

When M goes to infinity, at the tth user in the lth cell, the MMSE estimator can be written as

$$\hat{\boldsymbol{h}}_{ll_t} = \sqrt{\frac{\rho_0}{\tau}} Y_{l_t} \left(S_n + \frac{\rho_0}{\tau} \sum_{i=1}^{L} \sum_{k=1}^{K} \phi_{i_k}^H T_{li_k} \phi_{i_k} \right)^{-1} \cdot \phi_{l_t}^H T_{ll_t}, \tag{7}$$

where

$$S_n = E\left[W_{i_k}^H W_{i_k} \right] = MI_\tau \tag{8}$$

and

$$T_{li_k} = E\left[\boldsymbol{h}_{li_k}^H \boldsymbol{h}_{li_k} \right] = E\left[\sqrt{\beta_{li_k}}^H \boldsymbol{g}_{li_k}^H \boldsymbol{g}_{li_k} \sqrt{\beta_{li_k}} \right] = M\beta_{li_k}. \tag{9}$$

Then, we can formulate the MSE as

$$\frac{1}{M} MSE(L, K, \rho_0, \cos\theta) = \frac{1}{M} E_H \left\| \boldsymbol{h}_{ll_t} - \frac{1}{\rho_0} \hat{\boldsymbol{h}}_{ll_t} \right\|^2$$

$$= \frac{1}{M} E\left[tr\left\{ \left(\frac{1}{\rho_0} \hat{\boldsymbol{h}}_{ll_t} - \boldsymbol{h}_{ll_t} \right)^H \left(\frac{1}{\rho_0} \hat{\boldsymbol{h}}_{ll_t} - \boldsymbol{h}_{ll_t} \right) \right\} \right]. \tag{10}$$

To simplify this equation, let $\hat{\boldsymbol{h}}_{ll_t} = Y_{l_t} R$, where

$$R = \sqrt{\frac{\rho_o}{\tau}} \left(S_n + \frac{\rho_0}{\tau} \sum_{i=1}^{L} \sum_{k=1}^{K} \Phi_{i_k}^H T_{li_k} \Phi_{i_k} \right)^{-1} \cdot \Phi_{l_t}^H T_{ll_t}. \tag{11}$$

Then, (10) can be rewritten as

$$
\begin{aligned}
\frac{1}{M}MSE\left(L, K, \rho_0, \cos\theta\right) &= \frac{1}{M}E\left[tr\left\{\left(\frac{1}{\rho_0}Y_{l_t}R - \boldsymbol{h}_{ll_t}\right)^H\left(\frac{1}{\rho_0}Y_{l_t}R - \boldsymbol{h}_{ll_t}\right)\right\}\right] \\
&= \frac{1}{M}tr\left\{\frac{1}{\rho_0^2}R^H E\left[Y_{l_t}^H Y_{l_t}\right]R - \frac{1}{\rho_0}R^H E\left[Y_{l_t}^H \boldsymbol{h}_{ll_t}\right]\right. \\
&\quad \left. - \frac{1}{\rho_0}E\left[\boldsymbol{h}_{ll_t}^H Y_{l_t}\right]R + E\left[\boldsymbol{h}_{ll_t}^H \boldsymbol{h}_{ll_t}\right]\right\} \\
&= \frac{1}{M}tr\{T_{ll_t} - \frac{1}{\sqrt{\rho_0\tau}}T_{ll_t}\Phi_{l_t}R\} \\
&= \frac{1}{M}tr\left(M\left(\beta_{ll_t} - \beta_{ll_t}\tau\right.\right. \\
&\quad \left.\left. \cdot \left(\tau + \frac{\rho_0}{\tau}\sum_{i=1}^{L}\sum_{k=1}^{K}\phi_{l_t}\phi_{i_k}^H\beta_{li_k}\phi_{i_k}\phi_{l_t}^H\right)^{-1}\cdot\beta_{ll_t}\right)\right) \\
&= \frac{\rho_0\sum_{i=1}^{L}\sum_{k=1}^{K}\cos^2\theta_{l_ti_k}\beta_{li_k}}{1 + \rho_0\sum_{i=1}^{L}\sum_{k=1}^{K}\cos^2\theta_{l_ti_k}\beta_{li_k}}\cdot\beta_{ll_t} \quad (12)
\end{aligned}
$$

where $\cos\theta_{l_ti_k}$ represents the non-orthogonality between the two pilot signals of the tth user at the lth cell and of the kth user at the ith cell, respectively. By expressing the channel estimation error with the parameters in (12), it is feasible to investigate impact of non-orthogonal pilot sequences in channel estimation. This allows one to choose the proper non-orthogonality and reduce the channel estimation error to an acceptable level. Note that for the orthogonal case ($\cos\theta = 0$), the right-hand side of (12) is exactly zero, which implies no distortion in channel estimation.

3.3. Throughput analysis

The per-cell net sum-rate $C_{net}^{op}(\boldsymbol{p})$ is defined as the amount of $C_{sum}^{op}(\boldsymbol{p})$ within the portion of the normalized coherence time except for the time spent in channel estimation, where $C_{sum}^{op}(\boldsymbol{p})$ is called the per-cell sum rate that is the average rate during the entire data transmission time. In the case of orthogonal pilot sequences, $C_{sum}^{op}(\boldsymbol{p})$ and $C_{net}^{op}(\boldsymbol{p})$ are given by

$$
C_{sum}^{op}(\boldsymbol{p}) = \frac{1}{L}\sum_{d=0}^{\log_3 L-1}L3^{-d}C_d^{op} = \sum_{d=0}^{\log_3 L-1}3^{-d}C_d^{op}, \quad (13)
$$

$$
C_{net}^{op}(\boldsymbol{p}) = \frac{N_{coh} - N_{op}}{N_{coh}}C_{sum}^{op}(\boldsymbol{p}), \quad (14)
$$

where C_d^{op} denotes the net throughput of each subcarrier for one user at the cell with the pilot reuse factor d. The rates $C_{sum}^{np}(\boldsymbol{p}_\tau)$ and $C_{net}^{np}(\boldsymbol{p}_\tau)$ for the non-orthogonal case can be written as

$$
C_{sum}^{np}(\boldsymbol{p}_\tau) = \frac{1}{L}\sum_{d=0}^{\log_3 L-1}L3^{-d}C_d^{np} = \sum_{d=0}^{\log_3 L-1}3^{-d}C_d^{np}, \quad (15)
$$

$$
C_{net}^{np}(\boldsymbol{p}_\tau) = \frac{N_{coh} - \tau}{N_{coh}}C_{sum}^{np}(\boldsymbol{p}_\tau). \quad (16)
$$

Note that, under an optimization strategy for net-sum rates, non-orthogonality makes C_d^{np} is less than C_d^{op}. Nevertheless, when there are not sufficient communication time resources, it is possible to exploit the non-orthogonal features as the key point to attaining an enhanced net-sum rate. Fig. 3 shows a difference between the orthogonal and the non-orthogonal cases in pilot assignment. Instead of allowing non-zero but not so large non-orthogonality, the overall performance can be improved by securing a much larger number of sequences and reducing pilot reuse between nearby cells.
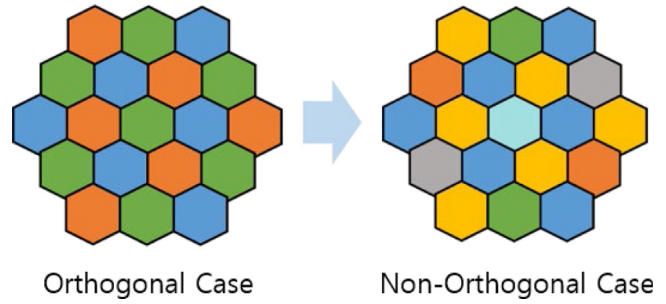

Fig. 3. Difference in pilot assignment for orthogonal and non-orthogonal pilot sequence sets.

4. Pilot optimization

According to [8], a transition vector $\boldsymbol{t} = (t_0, t_1, \ldots, t_{\log_3 L-2})$ corresponding to an assignment vector $\boldsymbol{p}$ can be defined as

$$
t_d = \begin{cases} t_0 = 1 - p_0 \\ t_d = -p_d + 3t_{d-1}, & 1 \le d \le \log_3 L - 2 \end{cases} \quad (17)
$$

where t_d is the number of transitions at depth d in the full pilot reuse state. Then, (13) is written as:

$$
C_{sum}^{op}(\boldsymbol{p}) = C_{sum}^{op}(\boldsymbol{t}) = KC_0 + \sum_{d=0}^{\log_3 L-2}t_d 3^{-d}(C_{d+1} - C_d) \quad (18)
$$

Note that the pilot assignment strategy in [19,20] was developed to maximize the term $\sum_{i=0}^{\log_3 L-2}t_d$, by using that $C_{d+1}^{op} - C_d^{op}$ is a constant. In a similar approach, we start our optimization process for the non-orthogonal case by checking whether the difference $C_{d+1}^{np} - C_d^{np}$ becomes a constant for applying non-orthogonal sequences to the assignment strategy. Taking into account the pilot contamination in L cells, the net throughput C_d^{np} [21] for a target user is computed as

$$
C_d^{np} = \log_2(1 + SIR_d) = \log_2\left(1 + \frac{\beta_{ll_t}^2}{OI_d + NI_d}\right), \quad (19)
$$

where SIR_d is the SIR of a user at depth d. Moreover, $OI_d = E_H\left\|\sum_{i=1}^{L3^{-d}-1}\beta_{li_t}^2\right\|$ and $NI_d = E_H\left\|\sum_{i,k=1}^{LK-(L3^{-d}-1)}\cos^2\theta_{l_ti_k}\beta_{li_k}^2\right\|$ represent pilot contamination from users with the same pilot sequences, and from users with different pilot sequences, respectively. The relationship between OI and NI in depths d and $d+1$ can be expressed as

$$
OI_{d+1} \approx \frac{1}{3 \times 4^\gamma}OI_d, \quad (20)
$$

$$
N_{d+1} - N_d = E_H\left\|\sum_{i,k=1}^{\frac{2}{3}L3^{-d}}\cos^2\theta_{l_ti_k}\beta_{li_k}^2\right\| \quad (21)
$$

where γ is the signal-decay exponent. Then, we can infer that $C_{d+1}^{op} - C_d^{op}$ approaches to a constant from (20). Note that (21) is the difference between the two pilot contamination values, which is approximately zero. We have

$$
\begin{aligned}
C_{d+1}^{np} - C_d^{np} &\approx \log_2\left(\frac{OI_d + N_d}{OI_{d+1} + N_{d+1}}\right) \\
&= \log_2\left(\frac{3*4^\gamma\left(1 + \frac{N_d}{OI_d}\right)}{1 + 3*4^\gamma\frac{N_{d+1}}{OI_d}}\right) \\
&\approx 0 \quad (22)
\end{aligned}
$$

because $3 * 4^\gamma \frac{NI_{d+1}}{OI_d} \gg 1$ and $NI_d/OI_d \gg 1$ in high-dense network scenarios. Thus, the pilot assignment strategy in (6) for orthogonal pilot signals can be valid in the non-orthogonal pilot cases. The interference from non-orthogonality, N_d, becomes dominant, even when the interference from pilot reuse, OI_d, decreases. Thus, $C_{d+1}^{np} - C_d^{np} \approx 0$ means that there is no remarkable change in terms of net throughput when the pilot reuse factor increases. That is, when the distance between cells with the same pilot sequence is increased by adopting a larger value of τ, the impact of pilot contamination of non-orthogonal pilot sequences from the adjacent cells is not suppressed.

By contrast, a lower channel estimation error should be guaranteed in view of the channel reliability for each transmission. It is required to analyze how the length of pilot sequences affects to the channel estimation, to formulate the minimal length of pilot sequences that maximizes the net-sum rate within the range of allowed channel estimation error. The Zadoff–Chu (ZC) sequence set [23], which satisfies the Welch bound [24] with equality, is one of the most widely used sequences for channel estimation. The ZC sequence set can maximize the number of users under a given pilot sequence length, and so it is appropriate to select this set as the pilot sequence set to maximize the net-sum rate. It has been also generally adopted in LTE systems [25]. The mathematical formulation of a ZC sequence set of length τ is given by

$$\phi_\mu = \left\{ \phi_\mu(n) = \exp\left(-\frac{j\pi\mu(n+1)}{\tau}\right), \quad 0 \le n \le \tau - 1 \right\}. \quad (23)$$

For the prime-length case, the number of distinct ZC sequences is

$$N_{np}(\boldsymbol{p}_\tau, \tau) = \tau^2 - \tau. \quad (24)$$

Furthermore, the pilot assignment vector can be formulated by

$$p_d^\tau = \begin{cases} \sum_{s=0}^d K3^s - \frac{(\tau-1)\tau - K}{2}, & d = x \\ 3\left(\frac{(\tau-1)\tau - K}{2} - \sum_{s=0}^{d-2} K3^s\right), & d = x+1 \\ 0, & \text{otherwise}, \end{cases} \quad (25)$$

where $x = \min\left\{ k \mid \sum_{s=0}^k K3^s > \frac{(\tau-1)\tau - K}{2} \right\}$. In the case $K = 1$, all the users can have distinct pilot sequences because the number of ZC sequences is large enough. Even in the presence of the interference arising from the non-orthogonality of pilot signals, the pilot contamination caused by pilot reuse is mitigated by increment of distance between cells sharing a pilot signal. The pilot contamination from pilot reuse can be minimized when the length of pilot sequences is prime, because the number of distinct sequences is maximized. Moreover, the non-orthogonality of ZC sequences becomes a constant $1/\sqrt{\tau}$. Then, the MSE can be reformulated as

$$\frac{1}{M} MSE(L, K, \rho_0, \tau) = \frac{\rho_0 \sum_{i \ne l}^L \sum_{k \ne t}^K \frac{\beta_{li_k}}{\tau}}{1 + \rho_0 \sum_{i \ne l}^L \sum_{k \ne t}^K \frac{\beta_{li_k}}{\tau}} \cdot \beta_{ll_t}. \quad (26)$$

From (26), we can observe that increase in τ gives reduction in channel estimation error. However, it is impossible to extending the pilot length because of the pilot overhead which is the ratio of spent time sending data to the coherence interval [21]. Specifically, if transition vectors $\boldsymbol{t}^1$ and $\boldsymbol{t}^2$ are generated from non-orthogonal sequences τ^1 and τ^2 of different lengths. Since $C_{d+1}^{np} - C_d^{np}$ approaches zero in a dense network, we have

$$C_{sum}^{np}(\boldsymbol{t}^1) - C_{sum}^{np}(\boldsymbol{t}^2)$$

$$= \left(KC_0 + \sum_{d=0}^{\log_3 L-2} t_d^1 3^{-d} \left(C_{d+1}^{np} - C_d^{np} \right) \right)$$

$$- \left(KC_0 + \sum_{d=0}^{\log_3 L-2} t_d^2 3^{-d} \left(C_{d+1}^{np} - C_d^{np} \right) \right)$$

$$\approx \left(t_{\log_3 L-2}^1 3^{-\log_3 L-2} \left(C_{\log_3 L-1}^{np} - C_{\log_3 L-2}^{np} \right) \right)$$

$$- \left(t_{\log_3 L-2}^2 3^{-\log_3 L-2} \left(C_{\log_3 L-1}^{np} - C_{\log_3 L-2}^{np} \right) \right)$$

$$\approx 0 - 0 = 0. \quad (27)$$

From (16) and (27), it is observed that a longer pilot length worsen the net-sum rate. In this perspective, we derive a minimal length of the pilot sequences under the constraint of MSE. Let $\overline{\tau}$ be a number satisfying $\frac{1}{M} MSE(L, K, \rho_0, \overline{\tau}) = \varepsilon$ for some $\varepsilon > 0$. The minimal length τ^* of the pilot sequences should satisfy the following three conditions:

(i) $\tau^* \ge \overline{\tau}$: This is clear from the constraint on MSE and the definition of $\overline{\tau}$.

(ii) $\tau^* \ge K$: To avoid intra-cell interference, pilot sequences should have a length larger than K.

(iii) τ^* is a prime number: For a ZC sequence set, the ratio of the number of distinct sequences to the length is $\tau - 1$, and less than $\sqrt{\tau}$ when τ is non-prime. A flowchart representing our optimization process is presented in Fig. 4.

5. Materials and methods

We assume the WINNER local area channel models under 5-GHz carrier frequency [26]. The normalized coherence time N_{coh} satisfies 1.7 µs/109 ns < N_{coh} < 17.4 µs/47.3 ns. In addition, γ, the signal decay exponent is 3.7, and the $SINR$ of the received pilot signal is 28 dB. As in Section 4, the non-orthogonal pilot set is selected as the ZC sequence set. The numerical calculation from the Eq. (26) indicates that $\tau^* \ge 16.492$ with $\varepsilon = 0.05$. To examine the net-sum rates over variable numbers of users within a cell up to $K = 19$, the minimal pilot length τ^* is set to 19. Note that $\boldsymbol{p}$ and $\boldsymbol{p}_\tau$ come from (6) and (25) for orthogonal and non-orthogonal cases, respectively.

5.1. Performance comparison for the number of users

Given $N_{op}(\boldsymbol{p}) = 51, L = 81$, and $\tau = 19$, Fig. 5 shows the comparison results between $C_{net}^{np}(\boldsymbol{p}_\tau)/K$ and $C_{net}^{op}(\boldsymbol{p})/K$ for $N_{coh} = 60, 90$ and 120. The simulation results show that a non-orthogonal case have a remarkable performance gain compared to a orthogonal case according to the increment of the number of users. The performance gap is larger for the smaller coherence time. In particular, when $K = 19$, $C_{net}^{np}(\boldsymbol{p}_\tau)/K$ is 45.95% (resp. 21.00%) higher than $C_{net}^{op}(\boldsymbol{p})/K$ for $N_{coh} = 90$ (resp. 120). Furthermore, $C_{net}^{op}(\boldsymbol{p})/K$ decreases more rapidly than $C_{net}^{np}(\boldsymbol{p}_\tau)/K$ when K increases. This result indicates that the use of the orthogonal pilot sequence set would worsen pilot contamination by reusing the same pilot signals, while the use of the non-orthogonal pilot sequence set can mitigate pilot contamination from the pilot reuse scheme by allocating distinct pilot sequences to users.

5.2. Performance comparison for the normalized coherence time

Fig. 6(a) illustrates $C_{net}^{np}(\boldsymbol{p}_\tau)/K$ for $K = 11, \tau = 19, 23, 31$ according to N_{coh}, Fig. 6(b) for $K = 17, \tau = 19, 29, 31$, and Fig. 6(c) for $K = 23, \tau = 23, 31, 37$. Performances with the non-orthogonal pilot sequence set are better than those with the orthogonal pilot sequence set when the coherence time is smaller than some specific values. The difference is because the length τ of the non-orthogonal pilot sequence is shorter than the length of the orthogonal pilot sequence under the same number of users. Furthermore, the higher the number of users, the higher
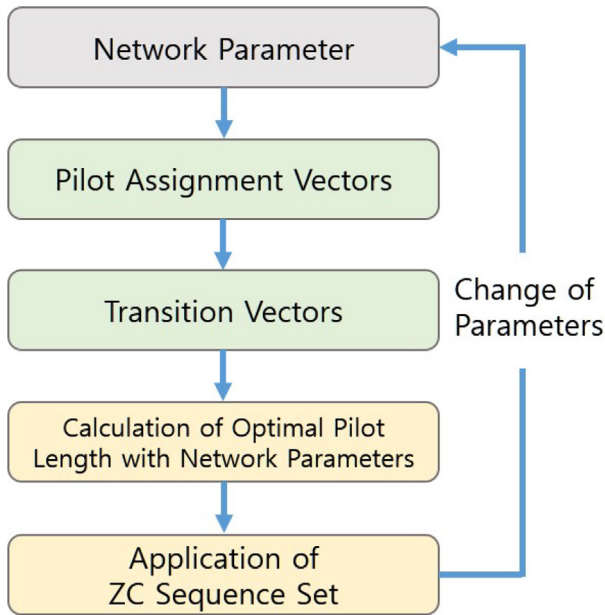
Fig. 4. Optimization process for non-orthogonal pilot sequences.

is the performance gap. By comparing of $C_{net}^{np}\left(\boldsymbol{p}_\tau\right)/K$s for distinct pilot lengths of non-orthogonal sequences, we observed that the highest net-sum rate is obtained when the shortest possible τ is used. Furthermore, the non-orthogonal pilot sequence set gives a lower variation of capacities over the change in N_{coh}, which implies that more stable capacities can be provided to users even when the velocity changes rapidly.

5.3. Variation in the size of pilot sequence sets

The tendency of net sum-rates in relation to the size of pilot sequence sets is shown in Fig. 7, for $K = 11, 17$, and $K = 19$. To prevent critical pilot contamination at the cell boundaries in a pilot reuse scheme, the size of the orthogonal pilot sequence set is often chosen by a number bigger than K. In the orthogonal case, the effect of over-allocation of pilot sequences is indicated by a decrease in the net throughput. In the orthogonal case with pilot reuse factors greater than or equal to one, the number of distinct orthogonal pilot sequences should be at least three times greater than K. In these cases, $C_{net}^{op}\left(\boldsymbol{p}\right)/K$ and $C_{net}^{np}\left(\boldsymbol{p}_\tau\right)/K$ show the results that the values are almost identical or that the non-orthogonal pilot sequence set is more advantageous than the orthogonal pilot sequence set.

6. Conclusion

In this study, we presented analysis and optimization scheme for non-orthogonal pilot sequence set in a multi-cell massive MIMO environment. We derived a certain condition for reducing the MSE for the non-orthogonal pilot sequences in channel estimation. Then, we formulated the minimal length of pilot signals under an allowable level of MSE. By simulation results, we demonstrated that a non-orthogonal pilot sequence set can deliver greater net-sum rates than an orthogonal pilot sequence set. This result shows that orthogonal pilot sequence set gives a remarkable improvements in throughput for environments comprising multiple users and low latency. In the future research, we will discover more advanced pilot assignment methods which are based on learning-based methods.
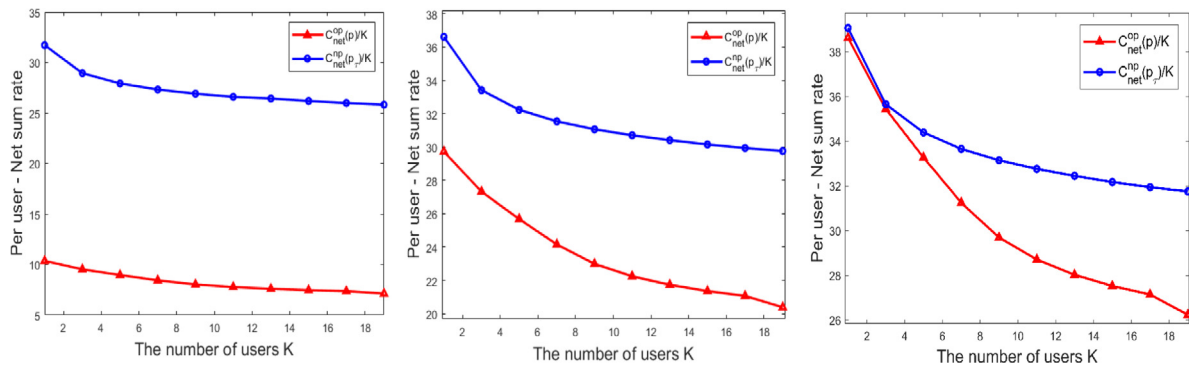

Fig. 5. Net throughput for the number of users K with $N_{op}(p) = 51, L = 81$ and $\tau = 19$ when the normalized coherence time is $60, 90$, and 120.

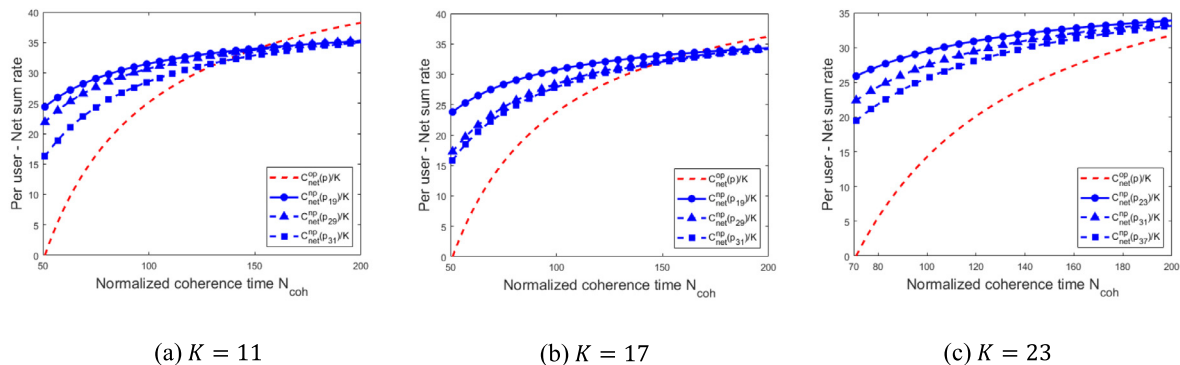(a) $K = 11$ (b) $K = 17$ (c) $K = 23$

Fig. 6. Net throughput for the normalized coherence time N_{coh} with (a) $=11, N_{op}(p) = 51, L = 81, \tau = 19, 23, 31$, (b) $K = 17, N_{op}(p) = 51, L = 81, \tau = 19, 29, 31$, and (c) $K = 23, N_{op}(p) = 71, L = 81, \tau = 23, 31, 37$.
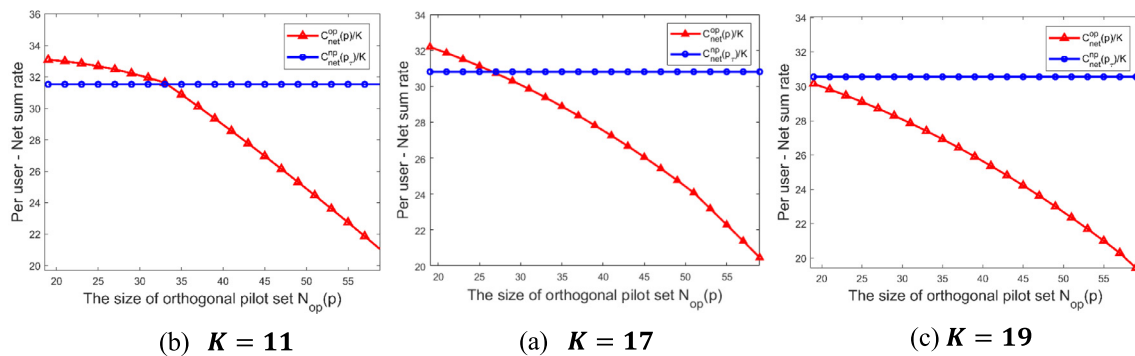
Fig. 7. Net throughput for the size of orthogonal pilot sequence sets $N_{op}(p)$ with $N_{coh} = 100$, $L = 81$ and $\tau = 19$ ($N_{np}(p_\tau, \tau) = 342$) when the number of users are **11, 17**, and **19**.

Declaration of competing interest

The authors declare that they have no known competing financial interests or personal relationships that could have appeared to influence the work reported in this paper.

Data availability

No data was used for the research described in the article.

References

[1] B.M. Hochwald, T.L. Marzetta, V. Tarokh, Multiple-antenna channel hardening and its implications for rate feedback and scheduling, IEEE Trans. Inform. Theory 50 (9) (2004) 1893–1909.
[2] Y. Léost, M. Abdi, R. Richter, M. Jeschke, Interference rejection combining in LTE networks, Bell Labs Tech. J. 17 (1) (2012) 25–49.
[3] J. Jose, A. Ashikhmin, T.L. Marzetta, S. Vishwanath, Pilot contamination and precoding in multi-cell TDD systems, IEEE Trans. Wirel. Commun. 10 (8) (2011) 2640–2651.
[4] T.X. Vu, A. Vu, T.Q.S. Quek, Successive pilot contamination elimination in multiantenna multicell networks, IEEE Wirel. Commun. Lett. 6 (3) (2014) 617–620.
[5] H. Wang, W. Zhang, Y. Liu, Q. Xu, P. Pan, On design of non-orthogonal pilot signals for a multi-cell massive MIMO system, IEEE Wirel. Commun. Lett. 4 (2) (2015) 129–132.
[6] X. Zhu, Z. Wang, L. Dai, C. Qian, Smart pilot assignment for massive MIMO, IEEE Commun. Lett. 19 (9) (2015) 1644–1647.
[7] X. Guo, S. Chen, J. Zhang, X. Mu, L. Hanzo, Optimal pilot design for pilot contamination elimination/reduction in large-scale multiple-antenna aided OFDM systems, IEEE Trans. Wirel. Commun. 15 (11) (2016) 7229–7243.
[8] N. Akbar, N. Yang, P. Sadeghi, R.A. Kennedy, Multi-cell multiuser massive MIMO networks: User capacity analysis and pilot design, IEEE Trans. Commun. 64 (12) (2016) 5064–5077.
[9] X. Zhu, Z. Wang, C. Qian, L. Dai, J. Chun, S. Chen, L. Hanzo, Soft pilot reuse and multicell block diagonalization precoding for massive MIMO systems, IEEE Trans. Veh. Technol. 65 (5) (2016) 3285–3298.
[10] J. Zuo, J. Zhang, C. Yuen, W. Jiang, W. Luo, Multicell multiuser massive MIMO transmission with downlink training and pilot contamination precoding, IEEE Trans. Veh. Technol. 65 (8) (2016) 6301–6314.

[11] S. Ma, E.L. Xu, A. Salimi, S. Cui, A novel pilot assignment scheme in massive MIMO networks, IEEE Wirel. Commun. Lett. 7 (2) (2018) 262–265.
[12] E. Björnson, J. Hoydis, L. Sanguinetti, Massive MIMO has unlimited capacity, IEEE Trans. Wirel. Commun. 17 (1) (2018) 574–590.
[13] Y. Wu, T. Liu, M. Cao, L. Li, W. Xu, Pilot contamination reduction in massive MIMO systems based on pilot scheduling, EURASIP J. Wirel. Commun. Netw. 21 (2018) 1–9.
[14] J. Fan, W. Li, Y. Zhang, Pilot contamination mitigation by fractional pilot reuse with threshold optimization in massive MIMO systems, Digit. Signal Process. 78 (2018) 197–204.
[15] W. Yuan, X. Yang, R. Xu, A novel pilot decontamination scheme for uplink massive MIMO systems, Procedia Comput. Sci. 131 (2018) 72–79.
[16] A.S. Al-hubaishi, N.K. Noordin, A. Sali, S. Subramaniam, A.M. Mansoor, An efficient pilot assignment scheme for addressing pilot contamination in multicell massive MIMO systems, Electronics 8 (4) (2019) 372.
[17] K. Shen, H.V. Cheng, X. Chen, Y.C. Eldar, W. Yu, Enhanced channel estimation in massive MIMO via coordinated pilot design, IEEE Trans. Commun. 68 (11) (2020) 6872–6885.
[18] F. Xu, H. Wang, H. Wang, H. Cao, Constellation coordination and pilot reuse for multi-cell large-scale MIMO systems, IET Commun. 14 (2) (2020) 357–363.
[19] J.Y. Sohn, S.W. Yoon, J. Moon, When pilots should not be reused across interfering cells in massive MIMO, in: Proc. IEEE Int. Conf. Commun. Workshop, ICCW, 2015, pp. 1257–1263.
[20] J.Y. Sohn, S.W. Yoon, J. Moon, On reusing pilots among interfering cells in massive MIMO, IEEE Trans. Wirel. Commun. 16 (2017) 8092–8104.
[21] T.L. Marzetta, Noncooperative cellular wireless with unlimited numbers of base station antennas, IEEE Trans. Wirel. Commun. 9 (11) (2010) 3590–3600.
[22] J. Amadid, M. Boulouird, M.M. Hassani, Channel estimation with pilot contamination in mutli-cell massive MIMO systems, in: 2020 IEEE 2nd International Conference on Electronics, Control, Optimization and Computer Science, ICECOCS, Kenitra, Morocco, 2020, pp. 1–4.
[23] D.C. Chu, Polyphase codes with good periodic correlation properties, IEEE Trans. Inform. Theory 18 (4) (1972) 531–532.
[24] L.R. Welch, Lower bounds on the maximum cross correlation of signals, IEEE Trans. Inform. Theory 20 (3) (1974) 397–399.
[25] M. Elsaadany, A. Ali, W. Hamouda, Cellular LTE-a technologies for the future Internet-of-Things: Physical layer features and challenges, IEEE Commun. Surv. Tutor. 19 (4) (2017) 2544–2572.
[26] T.A. Levanen, J. Pirskanen, T. Koskela, J. Talvitie, M. Valkama, Radio interface evolution towards 5G and enhanced local area communications, IEEE Access 2 (2014) 1005–1029.

Hong-Jae Lee received the B.S degree in electronic and control engineering from the Hanbat National University, Daejeon, South Korea, in 2019, and the M.S degree in electronic and computer engineering with the Communications and Code Design Laboratory from Ulsan National Institute of Science and Technology (UNIST), South Korea, in 2021. He is currently working as a researcher in Korea Telecom (KT). His research interests are massive MIMO 5G communication systems and machine learning for communications.

Dohyun Kwun received the B.S. degree in electrical engineering and mathematics from the Ulsan National Institute of Science and Technology (UNIST), South Korea, in 2019. He is currently pursuing the Ph.D. degree with Machine Intelligence and Information Learning laboratory, UNIST. His research interests include communication systems and reinforcement learning for communications.

Sung Whan Yoon received his B.S., M.S., and Ph.D. degrees in the Department of Electrical Engineering from Korea Advanced Institute of Science and Technology (KAIST), Daejeon, South Korea, in 2011, 2013 and 2017, respectively. He was a postdoctoral researcher at KAIST from 2017 to 2020. He is currently working as an Assistant Professor at AI Graduate School and the Department of Electrical Engineering at Ulsan National Institute of Science and Technology (UNIST), Ulsan, South Korea. His research interests are in communication & information theory, 6G intelligent communications, and deep-learning theory & algorithms. He was a co-recipient of the IEEE International Conference on Communications Best Paper Award in 2017.

Jin-Ho Chung received the B.S., M.S., and Ph.D. degrees from the Pohang University of Science and Technology (POSTECH), Pohang, South Korea, in 2005, 2007, and 2011, respectively. He was a Postdoctoral Researcher with the Communications and Signal Design Laboratory, Department of Electrical Engineering, POSTECH, from March 2011 to February 2013. From 2013 to 2020, he was an Assistant Professor at the Ulsan National Institute of Science and Technology (UNIST). From April 2013 to February 2014, he was a visiting Assistant Professor with the University of Waterloo. He is currently working as an Associate Professor with the School of IT Convergence at the University of Ulsan. His current research interests include information theory for machine learning, algebraic codes and sequences, and physical-layer security.

Seok-Ki Ahn received the B.S., M.S., and Ph.D. degrees in electronics and electrical engineering from the Pohang University of Science and Technology (POSTECH) in 2006, 2008, and 2013, respectively. From 2010 to 2013, he was a student on a scholarship at the Digital Media and Communications Research and Development Center, Samsung Electronics, Suwon, South Korea, where he was a Senior Engineer from 2013 to 2018. He is currently with Electronics and Telecommunications Research Institute (ETRI), Daejeon, South Korea. His research interests include channel coding, MIMO transceiver design, and broadband communications.